Granulometric stability of moraine embankment dam materials

Piezometric measurements in the core of dams made of moraines reveal that pore pressure dissipation mainly occurs near the downstream face of the cores, probably due to the lack of granulometric stability of these materials during seepage flow. To analyse this phenomenon, conventional criteria defining susceptibility to suffusion are first recalled and applied to the moraine materials composing the S. Valentino (Italy) and Suorva (Sweden) dams. An original numerical procedure to simulate the particle migration phenomena in granular media due to seepage processes is then reported. Effects of deposition–erosion processes occurred in the moraine materials composing the S. Valentino and Suorva dams, at the interface core–granular transition, have been then simulated and interpreted: the tolerable malfunctions (higher free surface profile and pore pressures) in the core of the S. Valentino dam and the failures at Suorva dams Paper by F. Federico and A. Montanaro

Moraine materials compose the core of several dams throughout the world, e.g. in the North of Italy (S. Valentino dam[1,2]), in Sweden[3] (Suorva dam[4,5]) or in the James Bay territory,[6] for their availability and ability to bear large strains, without hosting cavities or hollow fractures for a long time6, especially if characterized by low clay contents, moraine materials exhibit significant self-healing properties.

After some years of operation, these dams often show anomalies, high pore pressure and free surface profile in the core, pore pressure dissipation occurring near the downstream face of the core and in a thin zone of the material downstream of the core (filter or downstream shell), turbid water and leakages, rip-rap deformation, and sinkholes in the upstream shell.[7,8]

Moraine materials, in fact, are characterized by widespread grain size distribution (Figure 1), negligible cohesion, clay content and local heterogeneity; therefore, the finer fractions of these soils are susceptible to suffusion phenomena.[4,9,10,11,12]

The finer grains, under seepage forces depending on hydraulic gradients, may migrate through the voids bigger than their size, formed mainly by coarser particles. The drag forces may exceed the friction forces related to normal contact forces induced by their effective weight and confining pressures. The confining pressures are related to the effective stress state, which depends on the height of the dam, the geometry of the core, and the shape of the valley.

To safeguard the core (base *B*) material and avoid the progress of erosion, a protective transition (*T*) must be correctly designed[14]; its voids, related to the grain size distribution and porosity, must be sufficiently small to stop the migrating *B* particles within short distances, thus avoiding limit states related to backward erosion leading up to flow pipes generation; (*T*) must also allow a safe drainage of *B*, to avoid limit states as clogging and blinding, inducing in turn uncontrolled increases of pore pressures.

Figure 1. S. Valentino and Suorva dams. Grain size curves of the core materials and corresponding granular transitions.

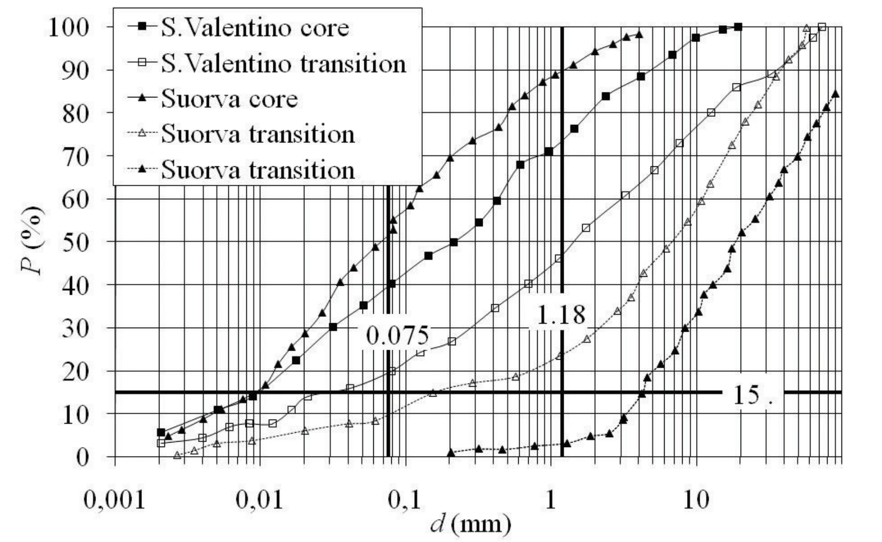

Problem setting

The core materials of the Suorva and S.Valentino dams, despite their comparable heights, physical and mechanical properties, behaved differently in operation. The Swedish dam suffered several accidents caused by the internal erosion processes (pipes, sinkholes, leakages...), while the Italian dam has operated efficiently since 1950, despite some minor and tolerable malfunction, specifically the higher free surface profile and pore pressures in the core, as compared to those expected in the original design.

The different behaviour of the two dams is analyzed by simulating the hydro-mechanical behaviour of the involved materials[17] through a

Figure 2: Problem setting. (1) One-dimensional unsteady seepage flow through a heterogeneous base (B) – transition (T) system; (2) B and T are divided into elements; (3) a constant total piezometric head difference ΔH is imposed.

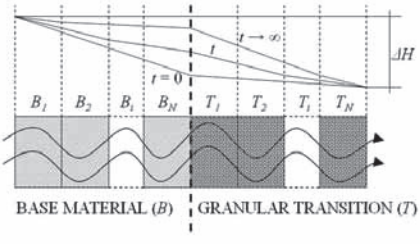

an advanced numerical procedure. Specifically, both spatial and time variations of the grain size, volume voids distributions and porosities[18] are simulated.

The adopted numerical procedure takes into account the grain size curve and the effective stress state, the hydraulic gradients and the flow velocities that, as a whole, influence the amounts of eroded fractions and the length of their migration paths.

Numerical procedure

Problem setting

Distributions of voids, constriction sizes and porosities of the granular material ("geometric-probabilistic models"[19,20,21,22]) have been coupled to the "hydraulic model"[23,24,25], to evaluate the rate of the seeping suspension, the piezometric gradients and the amounts of eroded/deposited granular fractions.

Movable particles may be eroded only if high hydraulic gradients or flow velocities, greater than their critical values, act (hydraulic condition) as well as if the particles cross voids greater that their sizes (geometrical condition).

The local variation of the grain size curve and porosity, due to the erosion/deposition of particles, modifies the volume voids distribution and permeability; so, flow rate, hydraulic gradients, drag and lift forces on migrating particles, the geometrical conditions (voids'sizes) change in space and time[23,26] too. The phenomenon evolves towards a stable condition (equilibrium) or an ultimate limit state (full erosion, clogging, blinding...).

To simulate this complex process, the *1D* unsteady seepage flow through a heterogeneous base (*B*) – transition (*T*) system, coupled with the migration of movable particles, induced by a constant, overall piezometric head difference Δ*H*, has been modeled and simulated.

Variable and governing equations

To better define the local hydraulic and geometric conditions, (*B*) and (*T*) have been decomposed into several elements (Figure 2), each characterized by initial grain size curve ($P_{j,0}$), porosity ($n_{i,0}$) and permeability ($k_{i,0}$); *i* and *j* define the system elements and materials granular fractions, respectively.

Figure 3. Forces acting on a migrating particle; a) plugged particle (d = d0); b) unplugged particle (d < d0); d, particle diameter; d0, average size of a pore channel.

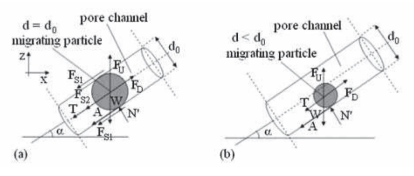

The variables $P_{j,t}$ and $n_{i,t}$ change during time due to the erosion-deposition processes; according to the Kozeny-Carman equation[27,28], $k_{i,t}$ changes too:

$$k_{i,t} = \chi \cdot \frac{\gamma_w}{\mu_w} \cdot \frac{n_{i,t}^3}{(1 - n_{i,t})^2} \cdot$$

γ_w being the water specific weight; μ_w, the water viscosity; d_h, the equivalent grains diameter; χ, a numerical coefficient.

The unsteady state is decomposed as a sequence of steady states, whose time interval is Δt ("successive steady states" method[27,29]); Δt may assume constant or variable value; for each Δt, the continuity equation holds:

$$\begin{vmatrix} \frac{k_{1,t}}{l_1} & \frac{k_{2,t}}{l_2} & 0 & L & L & 0 \\ 0 & \frac{k_{2,t}}{l_2} & -\frac{k_{3,t}}{l_3} & 0 & L & 0 \\ M & M & M & M & M & M \\ 0 & L & \frac{k_{1,t}}{l_1} & -\frac{k_{1+1,t}}{l_{i+1}} & L & 0 \\ M & M & M & M & M & M \\ 0 & L & L & 0 & \frac{k_{N-1,t}}{l_{N-1}} & \frac{k_{N,t}}{l_N} \\ 1 & 1 & L & L & L & 1 \end{vmatrix} \cdot \begin{pmatrix} \Delta h_{1,t} \\ \Delta h_{2,t} \\ M \\ \Delta h_{i,t} \\ M \\ \Delta h_{N,t} \end{pmatrix} = \begin{pmatrix} \\ \end{pmatrix}$$

Therefore, the suspension rate Q_t through the elements section Ω, and the volume of the granular suspension $V_{m,t}$, composed by the scoured particles dragged by the seeping fluid, entering and washed out from each element, is the same during each temporal step:

$$Q_t = \Omega \cdot k_{i,t} \cdot \frac{\Delta h_{i,t}}{l_i}; \quad V_{m,t} = Q_t \cdot \Delta t$$

So, the total volume of each element, composed of the original material ($V_{or,i,t}$), accumulated material ($V_{acc,i,t}$, $V_{acc,0} = 0$) and water saturating the i^{th} element ($V_{w,i,t}$), doesn't vary during Δ*t*.

The specific weight of filtering suspension is valued rearranging the equation proposed by Indraratna & Vafai[23]:

$$\gamma_{m_{i,t}} = \frac{\left(\frac{S_{acc_{t,i}}}{100} \cdot V_{acc_{i,t}} + \frac{S_{or_{i,t}}}{100} \cdot V_{or_{i,t}}\right) \cdot \gamma_{s_i} + V_{w_{i,t}} \cdot \gamma_w}{\frac{S_{acc_{i,t}}}{100} \cdot V_{acc_{i,t}} + \frac{S_{or_{i,t}}}{100} \cdot V_{or_{i,t}} + V_{w_{i,t}}}$$

$S_{acc,i,t}$ being the fraction of accumulated material scoured from the (i^{th}) element; $S_{or,i,t}$, fraction of the original material scoured from the (i^{th}) element, at time t. $S_{acc,i,t}$ and $S_{or,i,t}$ are computed through both hydraulic and geometric methods.

The particles can be scoured only if subjected to a flow velocity greater than the local, critical flow rate[24,28] (v_{cr}); v_{cr} is evaluated by analysing the forces acting on a movable particle and imposing its dynamic equilibrium along the flow direction.

A particle can migrate if the drag force F_D (Stokes law) exceeds the local shear resistance induced by the effective weight of the particle (*A*) and the confining stresses (F_S) (Figure 5): β being a coefficient that allows us to take into account the density of the granular matrix (0 < β< 4/π; β = 4/π for granular matrix composed by spherical particles arranged in hexagonal configuration, most dense state[25,28].

For a horizontal flow path, v_{cr} is expressed as:

$$v_{cr} = \frac{n}{3 \cdot \mu_w} \cdot \left[(\gamma_s - \gamma_w) \cdot \frac{d^2}{6} + \frac{\beta \cdot d}{2} \cdot (\sigma'_z + \sigma'_y)\right] \cdot \tan\varphi$$

$$v_{cr} = \frac{n}{3 \cdot \mu_w} \cdot \left[(\gamma_s - \gamma_w) \cdot \frac{d^2}{6}\right] \cdot \tan\varphi$$

The original material is generally subjected to strong confining actions (frictional forces, geometric hindrances); high values of the flow velocity need to mobilize the plugged particles. Conversely, the accumulated, unplugged particles, may be easily scoured during simulation; the corresponding critical flow velocity thus assumes small values (Equation 5).

The hydraulic conditions allowing the migration of movable particles are first considered; the analysis of the geometric conditions follows, if the previous one is verified ($v > v_{cr}$).

The particles (diameter d_j) composing the (i^{th}) element can be scoured only if they are able to cross through the voids of the $(i+1)^{th}$ element.

The statistical distributions of the pore volumes (V_j) and the corresponding constriction sizes, related to the geometry of the micro-configurations of suitably constrained granular masses composed of randomly disposed spheres (diameters d_j) are first theoretically determined.

The analysis is carried out through the Statistical Mechanics, by maximizing the configurational entropy associated with the distribution of these micro-variables[21,30,31].

The theoretical pore size distribution (PSD) curves is a function of the grain size $P_{j,t}$ and porosity $n_{i,t}$ of each element of the system.

The material scoured from the i^{th} element, at time *t* ($V_{s,out}$), depends on the specific weight of filtering suspension, γ_m[23]:

$$V_{s,out_{t,i}} = \frac{\gamma_{m_{t,i}} - \gamma_w}{\gamma_s - \gamma_w} \cdot V_{out,t}$$

The scoured volume of material is composed both by $V_{or,out}$ and $V_{acc,out}$ [18,32]:

$$V_{s,out_{i,t}} = V_{or,out_{i,t}} + V_{acc,out_{i,t}}$$

$$V_{accout_{i,t}} = \frac{V_{acc_{i,t}} \cdot S_{acc_{i,t}}}{V_{acc_{i,t}} \cdot S_{acc_{i,t}} + V_{or_{i,t}} \cdot S_{or_{i,t}}} \cdot V_{sout_{t,i}}$$

$V_{or,out}$ and $V_{acc,out}$ are decomposed into their granular fractions[23]:

$$\Delta V_{or,out_{t,j}} = V_{or,out_{i,t}} \cdot \frac{P_{or_{i,t,j}} - P_{or_{i,t,j-1}}}{S_{or_{i,t}}}$$

$$\Delta V_{acc,out_{i,t,j}} = V_{acc,out_{i,t}} \cdot \frac{P_{acc_{i,t,j}} - P_{acc_{i,t,j-1}}}{S_{acc_{i,t}}}$$

The element within which each scoured fraction is deposited, is determined through the corresponding length of the migration path, $L_{mig,j}$; this one depends on the probability of a particle not encountering a smaller constriction size.

The length covered by an assigned particle up to its arrest is finally based on concepts of stereology; it depends on the *PSD* as well as on the thickness of the filter[21,30,31].

The length of the migration path is then compared to the length that the particles can cross during each temporal step Δt:

$$L_{mig,j} = \min\lfloor s \cdot m_j;\ U_t \cdot \Delta t \rfloor$$

m_j being the number of constrictions greater than the particle size encountered by the particle along its path; *s* is the unit step assigned to each comparison.

At time $t + \Delta t$, the accumulated and original volume fractions within each element become:

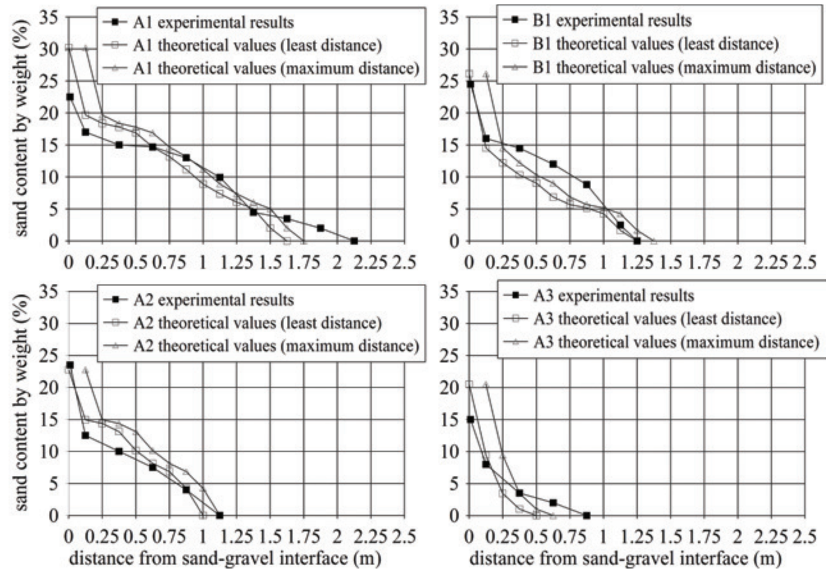

Figure 5. Sand content (s.c.) retained in the gravel at the end of each filtering process; theoretical vs experimental results: a) s.c. after 6,5 h (Sand A - Gravel 1); b) s.c. after 3 h (Sand B - Gravel 1); c) s.c. after 3,5 h (Sand A - Gravel 2); d) s.c. after 3,25 h (Sand A - Gravel 3).

$$\Delta V_{acc_{i,t+1,j}} = \Delta V_{acc_{i,t,j}} + \Delta V_{accin_{i,t,j}} - \Delta V_{accout_{i,t,j}}$$

$$\Delta V_{or_{i,t+1,j}} = \Delta V_{or_{i,t,j}} - \Delta V_{or,out_{i,t,j}}$$

This procedure allows for evaluation of the time evolution of the migration phenomena within granular media.

Validation of the numerical procedure

Theoretical analyses have been carried out first to validate the proposed numerical procedure by checking its ability to simulate the most significant laboratory tests results obtained by different authors through selected experiments on different materials.

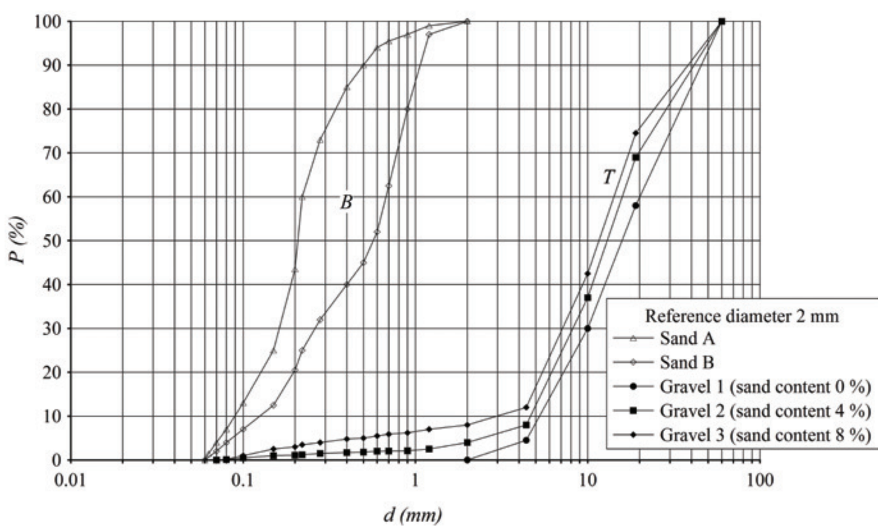

Figure 4. Grains size curves of involved materials22 (transition, T; base, B).

***Results by Atmazidis*[22]**

Atmazidis induced horizontal filtering processes, through materials at contact, sands (base, *B*) and gravels (transition, *T*) (Figure 4), by imposing a constant hydraulic gradient (i = 0.25). At the end of each test, the sand deposited within the gravels voids was measured.

The main features of the tests and the grain size curves of the involved materials are reported in Figure 4. The sand content retained in each gravel material, dragged from the *B* material, at the end of each filtering process, as a function of the distance from the interface among the two materials, is represented in Figure 5.

The particles migration phenomena observed by Atmazidis have been simulated according to the proposed numerical procedure. The whole thickness of the transition material (gravel), equals the experimental value 2.5m and it has been divided in 20 elements (each 12.5cm). The *B* material (sands) has been modeled as a single element (1m length); its erosion resistance has been neglected.

The computed values of the particles migration distances, larger for "clean" gravel (Gravel 1, 0% initial sand content) and smaller for gravels initially containing small sand content (Gravel 2 and Gravel 3) appreciably agree with the experimental ones (Figure 5).

Besides, the numerical procedure reproduces the "birth" of a filtering layer, at the interface *B-T*, which is able to avoid further sand erosion; the sand content in the first 5 - 7 cm of the gravels, after the sand-gravel interface, results extremely high (about 15 ÷ 25% by weight).

In the upstream zone of the gravels, a large amount of sand particles is deposited; this way, an effective filter layer, able to prevent further sand migration, is formed.

Figure 7:. Ratio Qt /Q0 versus time t (hours) (Q0, initial value of the suspension flow rate Qt) and particles accumulation in the protective transitions (d = 0.002 mm).S.Valentino Dam - Base and Transition: k0 = 1·10-6 m/s, n0 = 0.3, φ = 25.
Suorva Dam - Base: k0 = 1·10-6 m/s, n0 = 0.3, φ = 25; Finer Transition: k0 = 2.5·10-6 m/s, n0 = 0.3, φ = 25; Coarser Transition: k0 = 5·10-6 m/s, n0 = 0.3, φ = 25.

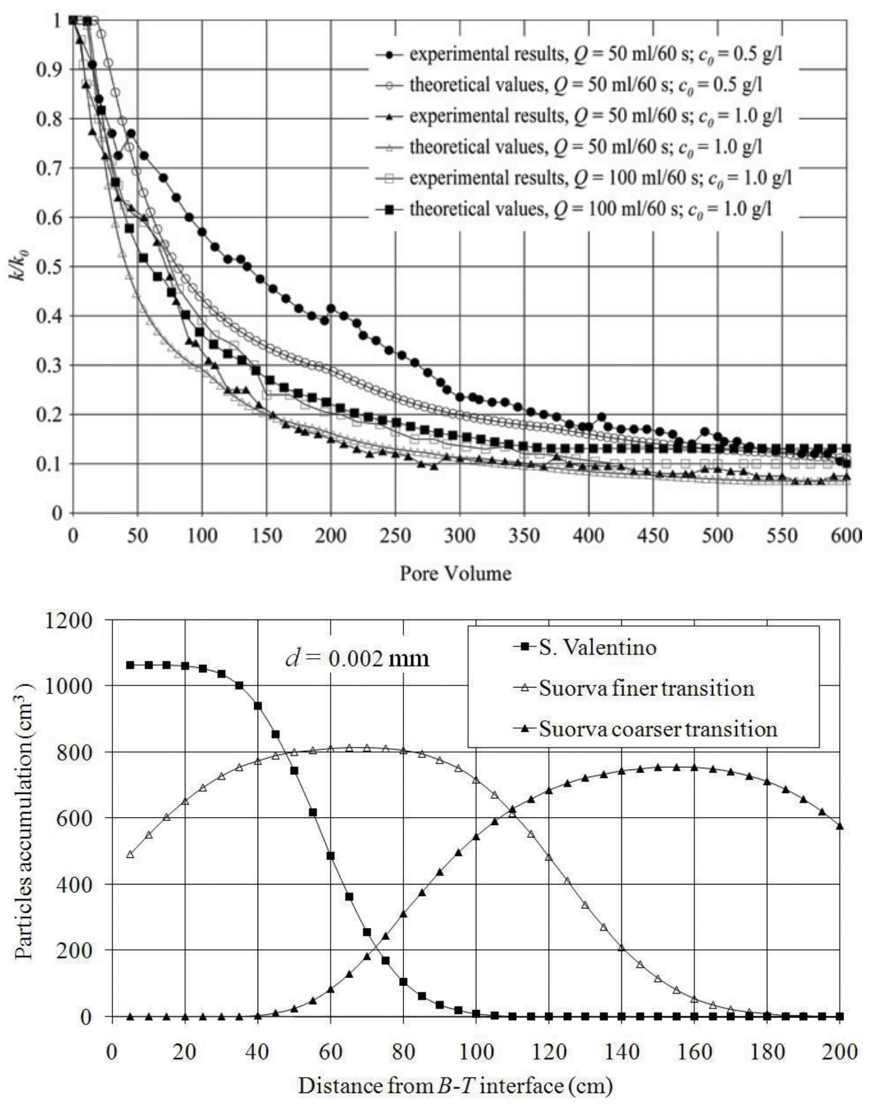

$$\Delta h_{i,t} = \frac{Q}{\Omega \cdot k_{i,t}} \cdot l_i$$

Besides, the theoretical results have been expressed in terms of the equivalent permeability, $k_{eq,t}$, of the element's series:

$$k_{eq,t} = \frac{L_{tot}}{\sum_{i=1}^{N_{el}} \frac{L_i}{k_{t,i}}}$$

c_0 affects the rate at which k decreases; the permeability of the filter decreases more quickly in the case of greater concentration. At the end of the tests, the permeability reduction attains nearly the same value ($k/k_0 = 0.1$) because, beyond a specific clogging state, flow velocities locally rise and particles deposition becomes negligible.

For the same reasons, greater values of Q produce similar results; greater velocities of the filtering suspension induce greater hydraulic forces; so, the deposition rate decreases, despite of a larger amount of injected material.

Results of simulations on moraine materials

Migration phenomena regarding the moraine materials of the S. Valentino and Suorva dams have been simulated through the proposed numerical procedure.

The length of the *B*-*T* systems is 3m (*B*: 1m, *T*: 2m); to simulate the displacements of the particles, from the *B* through the protective *T*, each system has been divided into 60 elements, 5cm length. The constant, overall piezometric head difference ΔH is equal to 6m; this value takes into account the available piezometric measures for the two dams. To promote their erosion, confining stresses on *B* particles are neglected (unplugged particles).

Results of numerical simulations show that erosion mainly involves the finer fractions ($d \approx$ 0.002mm) of the analyzed core materials. The ratio Q_t/Q_0 versus time t is shown in Figure 7 for the three analyzed case; Q_0 is the initial value of the suspension flow rate: Q_t/Q_0 rapidly increases if the Suorva core material is protected by the coarser transition, due to the intense erosion of the finer fractions of *B* and the corresponding increase of permeability.

After 12 hours, Q_t/Q_0 still increases: both granulometric and hydraulic stabilizations have not yet occurred. If the Suorva core material is protected by the finer transition, after four hours Q_t/Q_0 slowly decreases: the erosion of *B* is not still exhausted; the voids of *T* are progressively clogged, the process seems to reach a stable state.

The finer protective transition of S. Valentino dam controls the washout of the finer particles of *B*; Q_t very less increases respect to the Suorva analyzed cases. Stabilization occurs after six hours; Q_t becomes only 1.2 times greater than Q_0.

Results by Reddi[26]

Reddi measured the permeability reduction of a granular material due to the deposition of fine particles, suspended in a flowing liquid. Granular suspensions were composed by water and Kaolinite particles ($\gamma_S = 2650 kg/m^3$; two different values of concentrations c_0 (0.5 and 1 g/l) and imposed flow rate Q (50 ml/60s and 100 ml/60s) were considered in the tests. The particle suspension was injected in a cylindrical short column (1 –D flow, length $L = 64$mm, diameter $D = 76$mm), filled by sand ($k_0 = 3.6 \cdot 10^{-2}$cm/s; porosity $n_0 = 0.29$). The permeability (k) of this thin sample was indirectly computed by measuring the total head loss ΔH induced by the same sand filter:

$$K = \frac{4 \cdot Q \cdot L}{\pi \cdot \Delta H \cdot D^2}$$

Results (Figure 6) show the ratio k/k_0 vs the non dimensional ratio "Pore Volume" (PV). This ratio expresses the total volume of the injected granular suspension ($Q \cdot t$) divided by the initial volume of the voids of the sample ($n_0 \cdot \Omega \cdot L$):

$$PV = \frac{Q \cdot t}{n \cdot \Omega \cdot L}$$

PV represents an indirect measure of time, because the suspension rate *Q* has been maintained constant during each test; so, the injected volume linearly increases with the test duration.

To simulate the injection process (Q = const; q = Q/Ω) during time, the algebraic system (2) has been slightly modified:

The lengths of the path crossed by the eroded particles through the examined granular transitions (*T*) are very different (Figure 7). Within the *T* material of the S. Valentino dam, the maximum particles accumulation occurs just few cm after the *B-T* interface; in the finer transition material of Suorva dam, the maximum particles accumulation occurs about 70cm after the *B-T* interface; finally, in the coarser transition material of Suorva dam, about 150cm after the *B-T* interface.

Conclusions

An original numerical procedure to simulate the particle migration phenomena in granular media due to seepage flow, by taking into account constriction sizes and porosities of the particulate materials (geometric-probabilistic model) as well as the rate of the seeping suspension and piezometric gradients (hydraulic model).

The physical (porosity *n*) and hydraulic (permeability *k*) properties of the medium, during the coupled seepage flow, deposition and scouring particles processes, vary in the space, 1*D*, and along time, *t*.

Validation of the proposed method has been carried out by simulating selected experimental tests. Then, the granulometric stability of cohesionless moraine materials, composing the core of earth dams, has been analyzed. The migration process that takes place in proximity of the contact core–protective transition has been numerically simulated. Results put into evidence that the proposed numerical procedure allows to simulate the considered deposition–erosion process; specifically, erosion phenomena mainly involve the finer fractions of these materials and are not negligible and they may cause anomalies and malfunction, such as those ones often occurred in dams whose core is composed by broadly graded cohesionless materials protected by coarse granular transitions. ■

Acknowledgement

This article is based on a paper originally presented at the 6th International Conference on Dam Engineering, and was selected by the conference organisers for publication in IWP&DC. For more information visit http://dam11.lnec.pt

AUTHOR INFORMATION

F. Federico and A. Montanaro, University of Rome “Tor Vergata” , Via del Politecnico 1, 00133, Rome, Italy, email: fdrfnc@gmail.com

References

[1] P. Pinamonti, M. Scienza, A. Catalano, F. Del Gizzi, R. Jappelli, F. Federico and A. Montanaro, Safety of the San Valentino Dam after 60 Years of Operation, I.E.C.S. 2010, 643-648, Innsbruck, September 21-24, (2010).

[2] I.T.C.O.L.D. Materials for Earth and Rockfill Dams in Italy, Italian Committee on Large Dams (I.C.O.L.D.), Research Report n.2, November (1981) (in Italian).

[3] H.F. Rönnqvist, Evaluating internal instability and internal erosion in a selection of existing Swedish embankment dams, Internal Erosion of Dams and their Foundations - Fell & Fry (eds), Taylor & Francis Group, London, ISBN 978-0-415, (2007).

[4] Å. Nilsson, Filters and internal erosion in Swedish dams, Internal Erosion of Dams and their Foundations - Fell & Fry (eds), Taylor & Francis Group, London, ISBN 978-0-415, (2007).

[5] Å. Nilsson, The susceptibility of internal erosion in the Suorva Dam, Internal Erosion of Dams and their Foundations - Fell & Fry (eds), Taylor & Francis Group, London, ISBN 978-0-415, (2007).

[6] J. Lafleur, Internal stability of particles in dam cores made of cohesionless broadly graded moraines. Internal Erosion of Dams and their Foundations - Fell & Fry (eds), Taylor & Francis Group, London, ISBN 978-0-415, (2007).

[7] J. Laasonen, Internal Erosion and Duration of Grouting Works. Case History of a Small Embankment Dam, IECS2010, 409-412, Innsbruck, September 21-24 (2010).

[8] K. Radziki and S. Bonelli, A Possibility to Identify Piping Erosion in Earth Hydraulics Works Using Thermal Monitoring, IECS2010, 643-648, Innsbruck, September 21-24 (2010).

[9] R. Fell and J.J. Fry, The state of the art of assessing the likelihood on internal erosion of embankment dams, water retaining structures and their foundations, Internal Erosion of Dams and their Foundations - Fell & Fry (eds), Taylor & Francis Group, London, ISBN 978-0-415, (2007).

[10] R. Moffat, A laboratory study of particle migration in cohesionless soils, Master of Applied Science in the Faculty of Graduate Studies, University of British of Columbia, (2002).

[11] R. Fell, M. A. Foster and C.F. Wan, A framework for assessing the likelihood of internal erosion and piping of embankment dams and their foundations, Internal Erosion of Dams and their Foundations - Fell & Fry (eds), Taylor & Francis Group, London, ISBN 978-0-415, (2007).

[12] C.F. Wan and R. Fell, Investigation of internal erosion by the process of suffusion in embankment dams and their foundations, Internal Erosion of Dams and their Foundations - Fell & Fry (eds), Taylor & Francis Group, London, ISBN 978-0-415, (2007).

[13] R. Fell, C.F. Wan and M. A. Foster, Assessment of the likelihood on initiation of erosion in embankment dams, Internal Erosion of Dams and their Foundations - Fell & Fry (eds), Taylor & Francis Group, London, ISBN 978-0-415, (2007).

[14] F. Delgado, Tools for Assessing Granular Filters in Embankment Dams, European Working Group on Internal Erosion in Embankment Dams, Stockholm, September, (2006).

[15] M.A. Foster and R. Fell, Assessing Embankment Dam Filters That Do Not Satisfy Design Criteria, J. Geotech. Engrg., A..S.C.E., May, 398-407, (2001).

[16] J.L. Sherard and L. P. Dunnigan, Critical Filter for Impervious Soils, J. Geotech. Engrg., A..S.C.E., 115 (7), 546-566, (1989).

[17] G. Kampel, Mathematical modeling of fines migration and clogging in porous media, Thesis for the Degree Doctor of Philosophy in the School of Mathematics, Georgia Institute of Technology, December, (2007).

[18] A. Montanaro, Geotechnical design of granular transitions as protective filters. Thesis, University of Rome “Tor Vergata” (2006) (in Italian).

[19] A. Silveira, An analysis of the problem of washing through in protective filters, Proc. 6th Int. Conf. on Soil Mech. and Found. Engrg., Montreal, Vol. 2, 551-557, (1965).

[20] L. Wittmann, The Process of Soil-Filtration - its Physics and the Approach in Engineering Practice, 7th E.C.S.M.F.E., Vol.I, Brighton, 303-310, (1979).

[21] A. Musso and F. Federico, A geometrical probabilistic approach to the design of filters. Rivista Italiana di Geotecnica, Vol. XVII, n . 4, 173 – 193, (1983) (in Italian).

[22] D. K. Atmatzidis, A study of sand migration in gravel, 12th Int. Conf. On Soil Mech. and Found. Engrg.. Rio De Janeiro, Brazil, Session 8/3, pp. 683-686, (1989).

[23] B. Indraratna and F. Vafai, Analytical Model for Particle Migration Within Base Soil - Filter System. J. Geotech. Engrg., A..S.C.E., 123 (2), 100-109, (1997).

[24] S. Perzlmaier, Hydraulic criteria for internal erosion in cohesionless soil, Internal Erosion of Dams and their Foundations - Fell & Fry (eds), Taylor & Francis Group, London, ISBN 978-0-415, (2007).

[25] S. Biswas, Study of cohesive soil granular filter interaction incorporating critical hydraulic gradient and clogging, Engineering-Research Master, University of Wollongong, NSW, Australia (2005).

[26] L.N. Reddi, M. Xiao, M.G. Hajra and M. Lee, Permeability Reduction of Soil Filters due to Physical Clogging. J. Geotech. Engrg., A.S.C.E., 126 (3), 236-246, (2000).

[27] M. E. Harr, Groundwater and Seepage. Dover Publications Inc., (1962).

[28] G. Kovacs, Seepage hydraulics. Elsevier Publ., U.S.A. (1981).

[29] F.O. Franciss, Soils & Rocks Hydraulics. Fundamentals, Num. Meth. & Tech. of Electrical Analogs. Balkema, (1985).

[30] F. Federico and A. Musso, Some advances in the geometric-probabilistic method for filter design, Int. Conf. on “Filters and Filtration Phenomena in Geotechnical Engineering”, 75-82, Karlsruhe, October (1992).

[31] A. Musso and F. Federico, Pore size distribution in filtration analyses. XI I.C.S.M.F.E., S.Francisco, Vol. I, 1207-1212, (1985).

[32] F. Federico and A. Montanaro, Internal erosion in embankment dams. Phenomena, Lab. Experiments, Numerical Simulations, Colloquium Lagrangianum, February, Maratea, Italy (2009).

[33] R. Sakthivadivel, Theory and mechanism of filtration of non-colloidal fines through a porous medium, Tech. Rep. HEL 15-5, University of California, Berkeley (1966).